Geometric and Photometric Constraints for Surface Recovery

Jiping Lu Jim Little
Laboratory for Computational Intelligence
Department of Computer Science
The University of British Columbia
2366 Main Mall, Vancouver B.C., Canada V6T 1Z4

Abstract

In this paper we present a novel approach to surface recovery from an image sequence of a rotating object. In this approach, the object is illuminated under a collinear light source (where the light source lies on or near the optical axis) and rotated on a controlled turntable. A wire-frame of 3D curves on the object surface is extracted by using shading and occluding contours in the image sequence. Then the whole object surface is recovered by interpolating the surface between curves on the wire-frame. The interpolation can be done by using geometric or photometric methods. The photometric method uses shading information and is more powerful than geometric methods. The experimental results on real image sequence of matte and specular surfaces show that the technique is feasible and promising.

1 Introduction

An important task in computer vision is surface shape recovery from one or more 2D images. The recovered surface shape can be used in many applications, for example, localization, recognition, surface inspection in industry as well as 3D visualization and animation in Computer Graphics. Surface recovery from a single image is very difficult, requiring strong assumptions and sophisticated mathematical methods [2]. The results are usually not accurate and reliable. Surface recovery from multiple images taken by changing viewing directions (geometric stereo) or by changing illuminating directions (photometric stereo) gives better results. To change viewing directions, we can move the camera or, equivalently, change the orientation of the object. To move the camera, we usually have to perform calibrating to determine the precise location of the camera. Thus it is natural to consider rotating an object in front of a fixed camera. In photometric stereo, to recover the surface orientation of a whole object, Woodham [10] uses a rotary table to rotate the object. In shape from rotation [5, 6], Szeliski places an object on a spring-wound microwave turntable and uses optical flow information or contour information to derive the 3D structure of the object. In 3D model acquisition [11], Zheng puts an object on a turntable or a person on a swivel chair and uses contour information to extract a 3D model. In his recent work [12], Zheng uses specular motion of a rotating object for surface recovery. Although there are different kinds of information available, such as shading, contour, optical flow and stereo disparity, from the rotation of an object, the works mentioned above just use one of them.

In this paper, we propose a new technique which extracts a 3D wire-frame of the object surface from its image sequence using geometric and photometric constraints and then interpolates the surface points and normals between the curves on the wire-frame by using geometric methods or photometric methods [3]. The new technique does not require the object rotationally symmetric. It does not need surface reflectance function for extracting a wire-frame. Moreover the technique makes it possible to deal with piecewise uniform objects by extracting local reflectance function from the wire-frame and then applying the local reflectance function for local surface recovery.

2 Assumptions and Constraints

2.1 Experimental setup

The imaging facilities are placed in a dark room with black curtains. The imaging geometry is shown in Fig. 1. The object is on a turntable whose rotation angle can be precisely controlled. The Y axis coincides with the rotation axis of the turntable. A *collinear* light source, which points in the same direction as the camera viewing direction, and lies on or very near the optical axis, gives a uniform irradiance over the object. Since the camera is far away from the object, orthographic projection is used. A very simple calibration method is used to obtain the projection of the rotation axis in the images. Images are

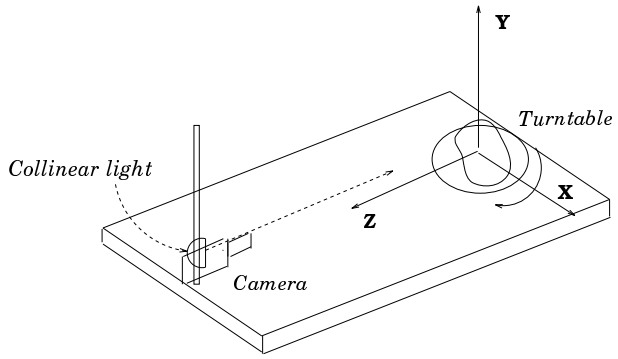

Figure 1: Experimental setup

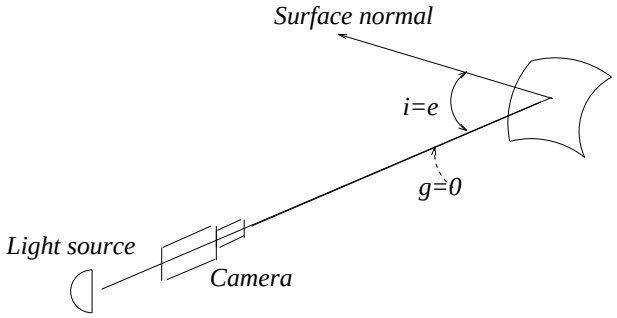

Figure 2: Under collinear light, the image brightness only depends on angle i

taken when the object rotates. The actions of taking images and rotating the object are synchronized by a computer program.

2.2 Geometric constraints

The object surface is assumed to be piecewise continuous and differentiable. The surface orientation is defined as $(p, q, 1)$ with $p = \partial z(x,y)/\partial x$ and $q = \partial z(x,y)/\partial y$. When an object rotates, the coordinates (x, y, z) and the orientation $(p, q, 1)$ of a surface point on the object change. After an α degree rotation, the 3D location of this point $(x_\alpha,\ y_\alpha,\ z_\alpha) = (x\cos\alpha - z\sin\alpha,\ y,\ x\sin\alpha + z\cos\alpha)$ and the surface orientation $(p_\alpha, q_\alpha, 1)$ of this point is determined by

$$p_\alpha = \frac{p\cos\alpha + \sin\alpha}{\cos\alpha - p\sin\alpha}, \quad (1)$$

$$q_\alpha = \frac{q}{\cos\alpha - p\sin\alpha}. \quad (2)$$

2.3 Photometric constraints

We also assume the reflectance of the object surface is uniform. This assumption can be relaxed to surfaces of piecewise uniform reflectances. In the general case, the image brightness of a 3D point under a distant light source is determined by the reflectance function $R(i, e, g)$ [9], where the incident angle i is the angle between the incident ray and the surface normal, the emergent angle e is the angle between the emergent ray and the surface normal, and the phase angle g is the angle between the incident and emergent rays. Under a collinear light source, as shown in Fig. 2, the phase angle g becomes zero and the incident angle i becomes the same as the emergent angle e. In this case, all the components of the reflectance such as the specular component, diffuse component and other components [7] are functions of the incident angle i only. Thus for the surface point (x, y, z), its image brightness value can be written as

$$E(x, y) = R(i(x, y)) \quad (3)$$

where $i(x, y)$ is the incident angle at point (x, y, z).

3 Wire-frame

When an object rotates in front of a camera, the contour information in images directly reflects the shape of the object and is more reliable than the other information. Under the illumination of a collinear light source, shading also provides information about incident angle. Integrating contour and shading, we can extract a wire-frame of 3D curves from images of a rotating object.

3.1 Equi-brightness constraint on surface points of $p = 0$

The surface reflectance in Equation 3 can be rewritten as $E = Q(\cos i(d))$. Here $i(d)$ is the incident angle of surface point d. Letting the p component of surface orientation at point d be zero, then $\cos i(d) = 1/\sqrt{q^2(d)+1}$. From now on, the subscript α will denote variables after an α degree rotation of the object. From Equation 1-2, we have $p_\alpha(d) = \frac{\sin\alpha}{\cos\alpha}$, $q_\alpha(d) = \frac{q(d)}{\cos\alpha}$ and

$$\begin{aligned}\cos i_\alpha(d) &= \frac{1}{\sqrt{p_\alpha^2(d)+q_\alpha^2(d)+1}} = \frac{\cos\alpha}{\sqrt{q^2(d)+1}} \\ &= \cos i(d)\cos\alpha.\end{aligned}$$

Under a collinear light source, for a surface point d, if we rotate the object by α degrees, its image brightness value is $E_\alpha(d) = Q(\cos i(d)\cos\alpha)$ and if we rotate the object by $-\alpha$ degrees, its image brightness value is $E_{-\alpha}(d) = Q(\cos i(d)\cos -\alpha)$. Therefore

$$E_{-\alpha}(d) = E_\alpha(d).$$

The above equi-brightness constraint tells us that a surface point of $p = 0$ will give the same image brightness after an α degree rotation of the object as it dose after a $-\alpha$ degree rotation of the object. Extending the above result from points to a curve, we conclude that at every point on a surface curve of $p = 0$, the image brightness after the object has been rotated by an angle α is the same as that after the object has been rotated by an angle $-\alpha$.

3.2 Depth on a curve of $p = 0$

A surface point of $p = 0$ on an object will be a surface point of $p = \infty$ after a 90 degree rotation of the object. Under the orthographic projection, the image of a surface point of $p = \infty$ will be a contour point in an image if there is no occlusion. Since we know the projection of the rotating axis in the images images, the horizontal distance from a contour point to the projection of the axis can be measured. The distance gives the depth value for the corresponding surface point of $p = 0$. Since the y coordinate of a surface point stays the same in its images during rotation under orthographic projection, the image correspondence between a $p = 0$ point and its contour point can be easily determined. Moreover the q component of a surface point of $p = 0$ can be calculated from the tangent at the corresponding contour point. To determine the 3D location of a $p = 0$ curve, we still need to find the x coordinate of each point on the curve.

3.3 3D location of a $p = 0$ curve

The geometric constraint on a surface point of $p = 0$ is derived from the following calculation. Let (x, y, z) be a surface point on a $p = 0$ curve and assume the coordinates of y and z are known. Let x_α, y_α and $x_{-\alpha}, y_{-\alpha}$ be the image coordinates of point (x, y, z) after the object has been rotated by α or $-\alpha$ degrees, respectively. The coordinates of y_α and $y_{-\alpha}$ are the same under the orthographic projection. From rotational transformation, we have

$$z = \frac{x_\alpha - x_{-\alpha}}{2 \sin \alpha}$$

and

$$x_\alpha - x_{-\alpha} = 2z \sin \alpha. \quad (4)$$

The equation shows that the disparity $x_\alpha - x_{-\alpha}$ is determined by the depth value of z. To find x_α and $x_{-\alpha}$ for a surface point of $p = 0$, three images, the images taken after 90 degree, α and $-\alpha$ rotation, are used. By the epi-polar constraint, we only need to look at the images points in the same row of the three images. We get the depth value by measuring the horizontal distance from a contour point to the projection of the rotation axis in the image taken after 90 degree rotation and calculate the disparity. For every image point in the same row of the image taken after α degree rotation, we use the disparity to calculate its correspondence in the image taken after $-\alpha$ degree rotation and check if the two image correspondence have the same brightness value. If they have the same brightness value, the two image points are considered the projection of a $p = 0$ surface point. The search for the correspondence is linear and can be simplified by using results from adjacent rows.

After the values for x_α and $x_{-\alpha}$ have been obtained, the x coordinate of the surface point (x, y, z) can be determined by $x = \frac{x_\alpha + x_{-\alpha}}{2 \cos \alpha}$. The above search can be applied to every point on a curve of $p = 0$ to get the 3D location of the curve.

3.4 Wire-frame of curves of constant p

A curve of $p = tan\theta$ on an object surface can be transformed to a curve $p = 0$ by rotating the object by angle $-\theta$. So the 3D location as well as the surface orientation of a curve of $p = tan\theta$ can be determined by using the same method as we described above. Let $n = 360°/\theta$ and θ divide 90°, and let the images of the object be taken each time the object has rotated by angle θ. After the object has been rotated by 360 degrees, we can compute a set of curves of constant p from the image sequence. These curves comprise a wire-frame on the object surface. The depth and surface orientation between two adjacent curves on the wire-frame can be interpolated by using either geometric or photometric methods.

4 Experiments on a Matte Surface

4.1 Image sequence

In our experiment, we use a calibrated image facility (CIF) [10] built in our lab to control the object rotation and the imaging conditions. Thirty six images are taken during the 360 degree rotation of an object with 10 degree rotation for each image. The images are smoothed with a Gaussian filter of $\sigma = 1$ to filter noise and quantization effects. A clay ellipsoid is used for our first experiment. The surface of the ellipsoid can be consider a matte surface. Four images from the image sequence of the ellipsoid are shown in Fig. 3.

4.2 Extracting the wire-frame

To extract the $p = \tan\theta$ curve, three images taken after $(\theta + 90)$ *mod* 360 degree, $(\theta - \alpha)$ *mod* 360 degree, $(\theta + \alpha)$ *mod* 360 degree rotation are used. In our experiment, $\alpha = 20$. For example, to extract the $p = 0$ curve, the images taken after 90 degree, 20 degree and -20 degree rotation are used. These three images are shown in Fig. 4. The black vertical line in

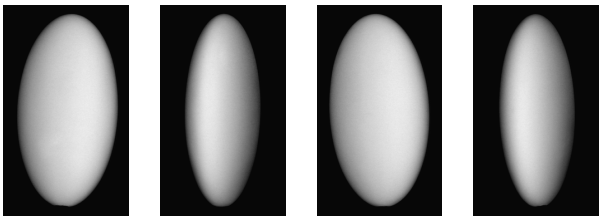

Figure 3: Images of a rotating ellipsoid

image (a) is the projection of the rotation axis. The white contour in image (a) is extracted by a simple thresholding method. The horizontal distance from each contour point to the projection of the rotation axis gives the depth value for the corresponding point on the $p = 0$ curve. The disparities of the image points of the $p = 0$ surface curve in image (b) and (c) are calculated by Equation 4. The projections of the $p = 0$ surface curve on image (b) and image (c) are determined by the searching method we described in the previous section. The black curve in image (d) is the projection of the $p = 0$ curve on the image taken before rotation. We extracted 36 curves of constant p from the image sequence. These curves comprise a wire-frame on the object surface. The projection of the wire-frame on the image taken before rotation is shown in Fig. 5 image (a).

4.3 Geometric interpolation

The p and q components of the surface orientation on the wire-frame are determined from the object rotation angle and the tangent at the contour points in the images. The surface orientation and depth values between the adjacent curves on the wire-frame are geometrically interpolated by using depth and orientation data on the wire-frame. The interpolation is implemented with graphics program Optik [1]. First we connect the areas between each two adjacent curves with triangles and get a mesh of the surface. Then we input the 3D coordinates and surface orientations of the vertices of the mesh to the program Optik. The program Optik does surface orientation interpolation and gives a shaded image of the recovered surface. In Fig. 5, image (b) is the ellipsoid reconstructed with a triangular mesh, while images (c) and (d) are the synthetic images of the recovered surface. The attitude of the ellipsoid in image (c) is the same as that in the image taken before object rotation. The viewing direction and light source direction used to generate image (c) are collinear so that we can compare the synthetic

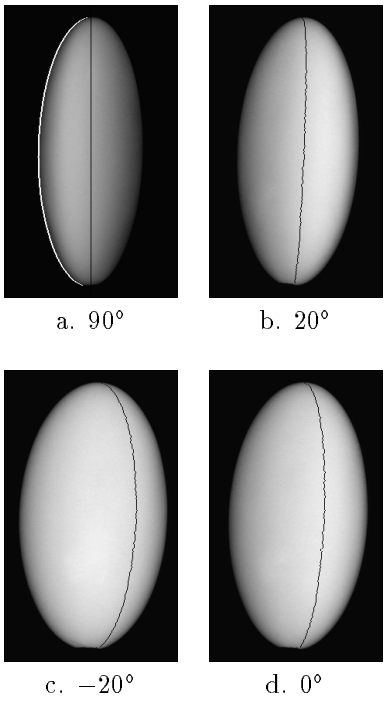

Figure 4: Extracting $p = 0$ curve from images a-c

image with the corresponding real image. The viewing and illuminant direction as well as the attitude of the ellipsoid for synthetic image (d) are different from those for the real images were taken.

5 Experiment on a Specular Surface

5.1 Wire-frame on a porcelain cup

We also experimented with a porcelain cup. The reflectance of the cup contains a strong specular component. Six images from the image sequence of the rotating cup are shown Fig. 6. Since the object is not a simple convex object, there is more than one $p = \tan\theta$ curve at any moment of the rotation. Three images, image (a), (b) and (c) in Fig. 7, are used to extract the $p = 0$ curves of the object. Image (a) shows the occluding contours in image after 90 degree rotation. These white curves are give depth values for the $p = 0$ curves. Images (b) and (c) in Fig. 7 are images taken after 20 degree and -20 degree rotation, respectively. In this experiment, both silhouettes and self-occluding contours are used. One of the contours in image (a) is a self-occluding contour and used to extract the $p = 0$ curve on the handle. Image (d) in Fig. 7 is the projection of the two $p = 0$ curves, which are extracted from images (a), (b) and (c). The other $p = \tan\theta$ curves are extracted in the same way. These extracted curves

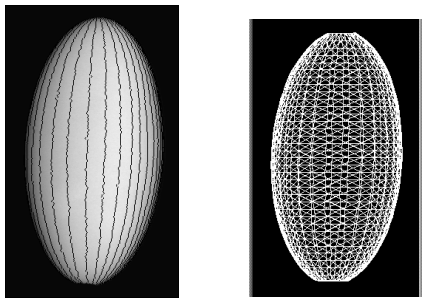

a. wire frame b. mesh

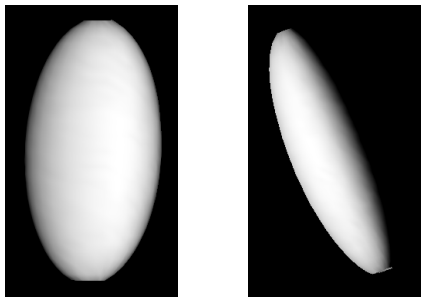

c. shaded image 1 d. shaded image 2

Figure 5: The recovered surface of the ellipsoid

comprise a wire-frame on the object surface. The projection of the wire-frame on images is shown in Fig. 8. From these images, we can see that the wire-frame is not complete. This is because the silhouettes in some images are occluded by the other part of the object so that only partial curves can be extracted. On one side of the cup, there is a pig figure on it. The protrusion and the color of the figure violates our uniform surface assumption so that the curves on the body part of that side cannot be extracted.

5.2 Photometric interpolation

Since the wire-frame on the cup surface is incomplete, some details of the surface will be lost in recovery if geometric interpolation is used. For example, there is not sufficient geometric information on the wire-frame to interpolate the joints between the handle and the body of the cup. The photometric interpolation described by Lu and Little [3] is used to overcome the problem. First the surface reflectance function of the cup is estimated by using the method described in [3]. Fig. 9 is the reflectance function extracted from the images of the rotating cup. In practice, the inverse function $i = R^{-1}(E)$ is used for surface recovery.

The photometric interpolation uses two images

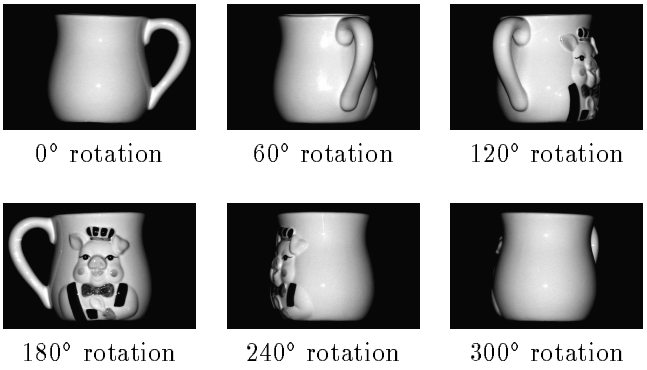

0° rotation 60° rotation 120° rotation

180° rotation 240° rotation 300° rotation

Figure 6: Images of a rotating cup

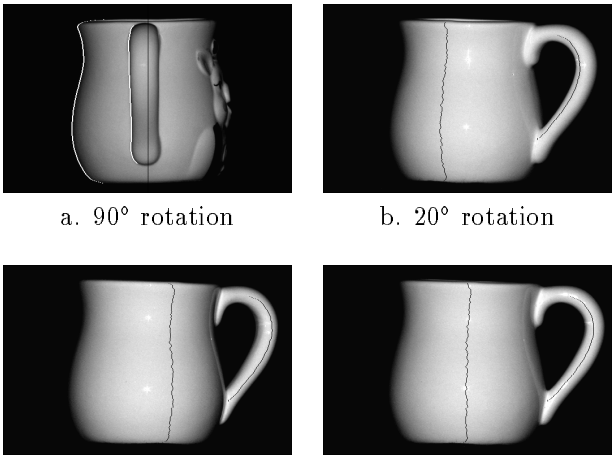

a. 90° rotation b. 20° rotation

c. $-20°$ rotation d. 0° rotation

Figure 7: Extracting $p = 0$ curves from images a-c

taken at different rotation angles of the object and recovers the depth and surface orientation at every pixel in one of the two images. The interpolation starts from image points of the wire-frame. Using the values of p ($p = \frac{\partial z}{\partial x}$) and z at an image point of the wire-frame, a new depth value z' for a neighbor point in the x direction can be calculated by $z' = z + pdx$. With the depth value of the neighbor point, its projections as well as its brightness values in the two images can be found. From the surface reflectance function and the two brightness values, the two incident angles of this neighbor point at the time the two images were taken can be estimated. Letting the two incident angles be i_0 and i_1, the p, q, component of the surface orientation for the neighbor point is computed by:

$$p = \frac{1}{\tan\alpha} - \frac{\cos i_1}{\cos i_0 \sin\alpha},$$

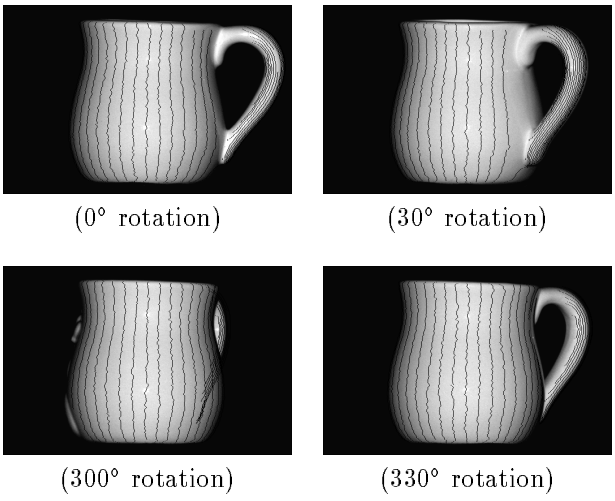

Figure 8: Projections of the wire-frame on images

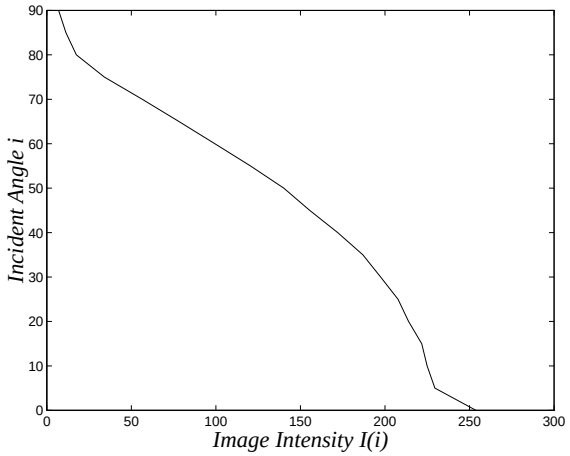

Figure 9: The reflectance function of the cup

and

$$q = \pm\sqrt{\frac{1}{\cos i_0^2} - p^2 - 1}.$$

The computation for depth and surface orientation can be expanded further by using the depth value and surface orientation of the neighbor point until an image point of another curve on the wire-frame is reached. In this way we obtain a set of depth values on a path which connects the two points on the wire-frame. Because of the accumulated error caused by image noise and other facts, the depth value calculated at the end point may not meet the depth value on the wire-frame. This will cause a discontinuity in the depth value. To overcome this problem, a *distance-weighted averaging* method is used [3]. The idea is that two sets of depth values on the path are computed. Each starts from one of the two end points of the path and ends at the other point. The final depth value of a point on the path is determined by averaging the two depth values. The depth value computed near its starting point is assigned with a larger weight; otherwise it is assigned with a smaller weight. In this way a continuous surface curve in the x direction can be constructed. Fig. 10 shows the surface height plot of the the recovered cup. The depth values are directly used for display without any smoothing or regularization.

6 Discussion and Future Work

From our experience and observations, we know that several factors cause errors in surface recovery. The interreflection between the different parts of the surface is one of them. Image noise is another, which causes non-smoothness of the $p = 0$ curves. Quantitation on the image brightness values and the coordinates in $x - y$ space also put a limit on the accuracy of the recovered surface.

The whole surface recovery process is not fully automatic yet. To extract the self-occluding contour, we have to pick a starting point for the contour extracting program. Also we have to do segmentation if a silhouette corresponds to the surface boundaries of two or more parts of the object. To improve our technique and to make the whole process automatic, we can use the silhouettes and occluding contours to find the enclosing volume of the object. From the enclosing volume, we can determine the topological relation between the different parts of the object and therefore extract and segment different occluding contours for the different parts.

One immediate extension of our wire-frame technique is to a piecewise uniform surface, such as a surface of different colors. To extract a wire-frame from the image sequence, the surface does not have to be uniform as long as the equi-brightness constraint holds when the object is viewed and illuminated from two symmetric directions. The surface depth and orientation information on the wire-frame can be used to compute a local reflectance function for each uniform region. Then the local reflectance function can be used for local photometric interpolation.

Currently, we can't recover the surface on the pig side of the cup. Integrating stereo information with photometric information is one way to solve this problem. Interreflection is usually hard but feasible in

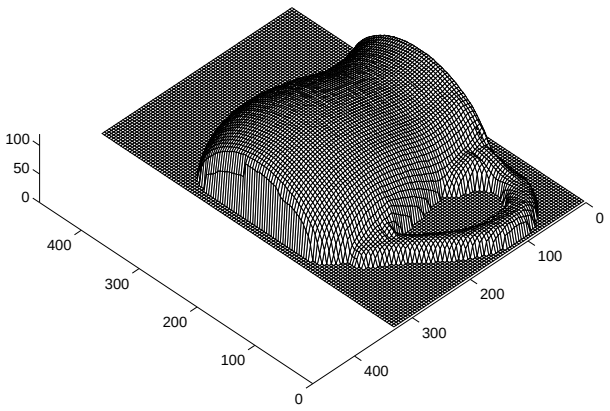

Figure 10: The height plot of the recovered cup

some conditions [4, 8]. We believe that under the collinear light source, the problem is well constrained since the surface reflectance function can be extracted from an image sequence and a relatively accurate initial surface can be estimated. Moreover the interreflection under the collinear light source is easy to analyze.

Compared to other techniques of surface recovery from image sequence of a rotating object [12, 11, 5, 6], our technique has certain advantages. First it does not require a continuous image sequence. Secondly it can get a dense map of both surface depth and orientation at the same time. Finally our technique works on any surface of isotropic reflectance function. The intended applications of our technique are automatic modeling in industry as well as in Computer Graphics.

7 Acknowledgments

We would like to thanks Jeffrey Beis and the others who offered help to our work. The author's email address are jplu@cs.ubc.ca and little@cs.ubc.ca. This research was supported by grants from the Natural Sciences and Engineering Research Council of Canada and the Networks of Centres of Excellence Institute for Robotics and Intelligent Systems, Projects A-1 and IS-6.

References

[1] J. Amanatides, J. Ruchanan, and *et al.* Optik user's manual, version 2.6. 1993.

[2] B. K. P. Horn and E. M. J. Brooks. *Shape from Shading.* (in press), MIT Press, Cambridge, MA, 1988.

[3] J. Lu and J. Little. Reflectance function estimation and shape recovery from image sequence of a rotating object. In *Proc. 5th International Conference on Computer Vision*, pages 80–86, 1995.

[4] S. K. Nayar, K. Ikeuchi, and T. Kanade. Shape from interreflections. *Int. J. Comp. Vision*, 6(3):173–195, 1991.

[5] R. Szeliski. Shape from rotation. In *CVPR-91*, pages 625–630, June 1991.

[6] R. Szeliski and R. Weiss. Robust shape recovery from occluding contours using a linear smoother. In *Image Understanding Workshop*, pages 939–948, Whshington, D. C., 1993.

[7] H. D. Tagare and R. J. deFigueiredo. A theory of photometric stereo for a class of diffuse non-Lambertian surfaces. *IEEE-PAMI*, 13(2):133–152, 1991.

[8] T. Wada, Y. Fukagawa, and T. Matsuyama. Shape from shading with interreflections under proximal light source: 3d shape reconstruction of unfolded book surface from a scanner image. In *Proc. 5th International Conference on Computer Vision*, pages 66–71, 1995.

[9] R. J. Woodham. Photometric method for determining surface orientation from multiple images. *Opt. Eng.*, 19:139–144, 1980.

[10] R. J. Woodham. Gradient and curvature from photometric stereo including local confidence estimation. *J. Opt. Soc. Amer.*, 11(11):3050–3068, Nov. 1994.

[11] J. Y. Zheng. Acquiring 3-D models from sequences of contours. *IEEE-PAMI*, 16(2):163–178, 1994.

[12] J. Y. Zheng, Y. Fukagawa, and N. Abe. Shape and model from specular motion. In *Proc. 5th International Conference on Computer Vision*, pages 72–79, 1995.